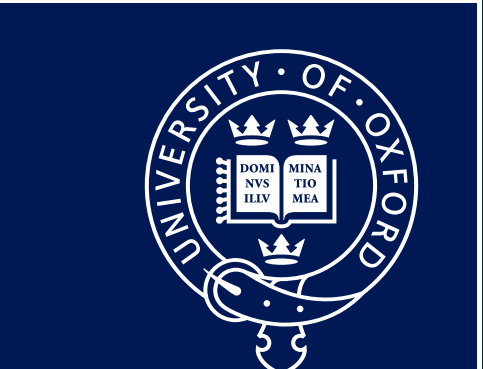


The Structure and Properties of Endohedral Clusters Containing a Transition Metal Dimer Core, $M_2 E_{12}$.



UNIVERSITY OF
OXFORD

Ya-Nan Yang,^{b+} Zisheng Li,^{a*} Lei Qiao,^b Cui-Cui Wang,^b Wen-Juan Tian,^b Sourav Mondal,^a Zhong-Ming Sun,^{b*} and John E. McGrady.^{a*}

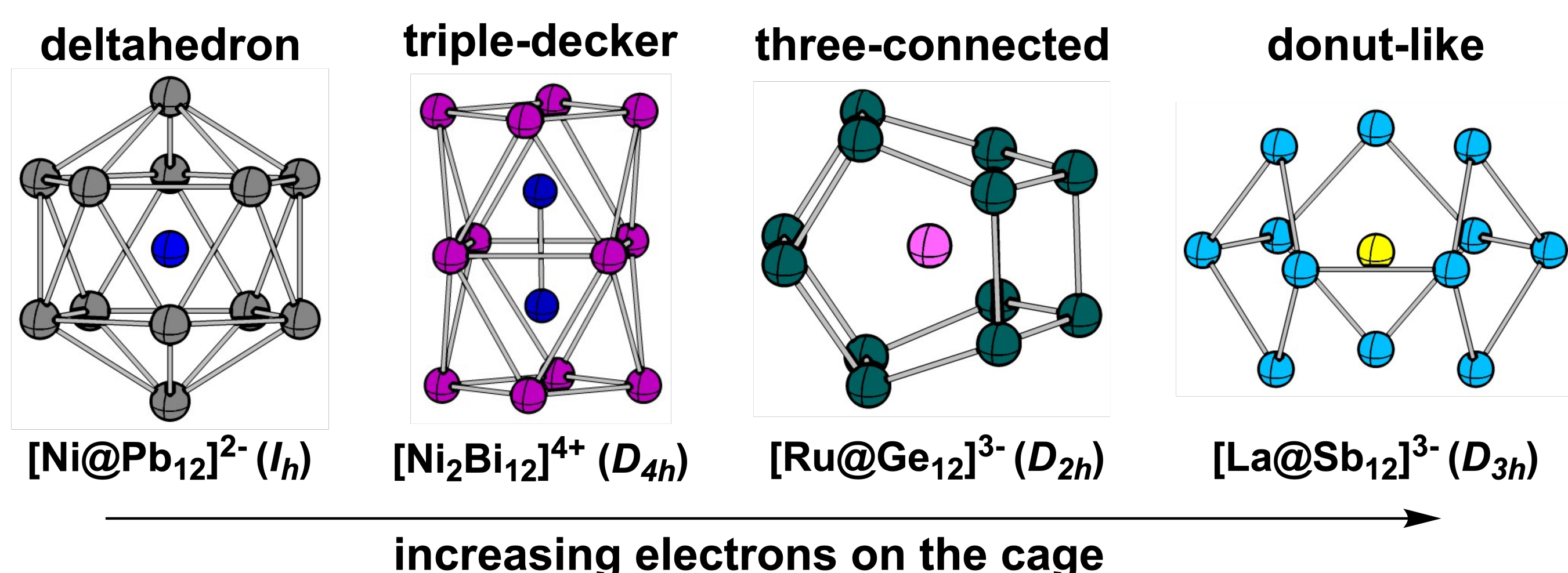
a. Department of Chemistry, University of Oxford, Oxford OX1 3QR, UK

b. State Key Laboratory of Elemento-Organic Chemistry, Tianjin Key Lab for Rare Earth Materials and Applications, School of Materials Science and Engineering, Nankai University, Tianjin 300350, China.

zisheng.li@chem.ox.ac.uk

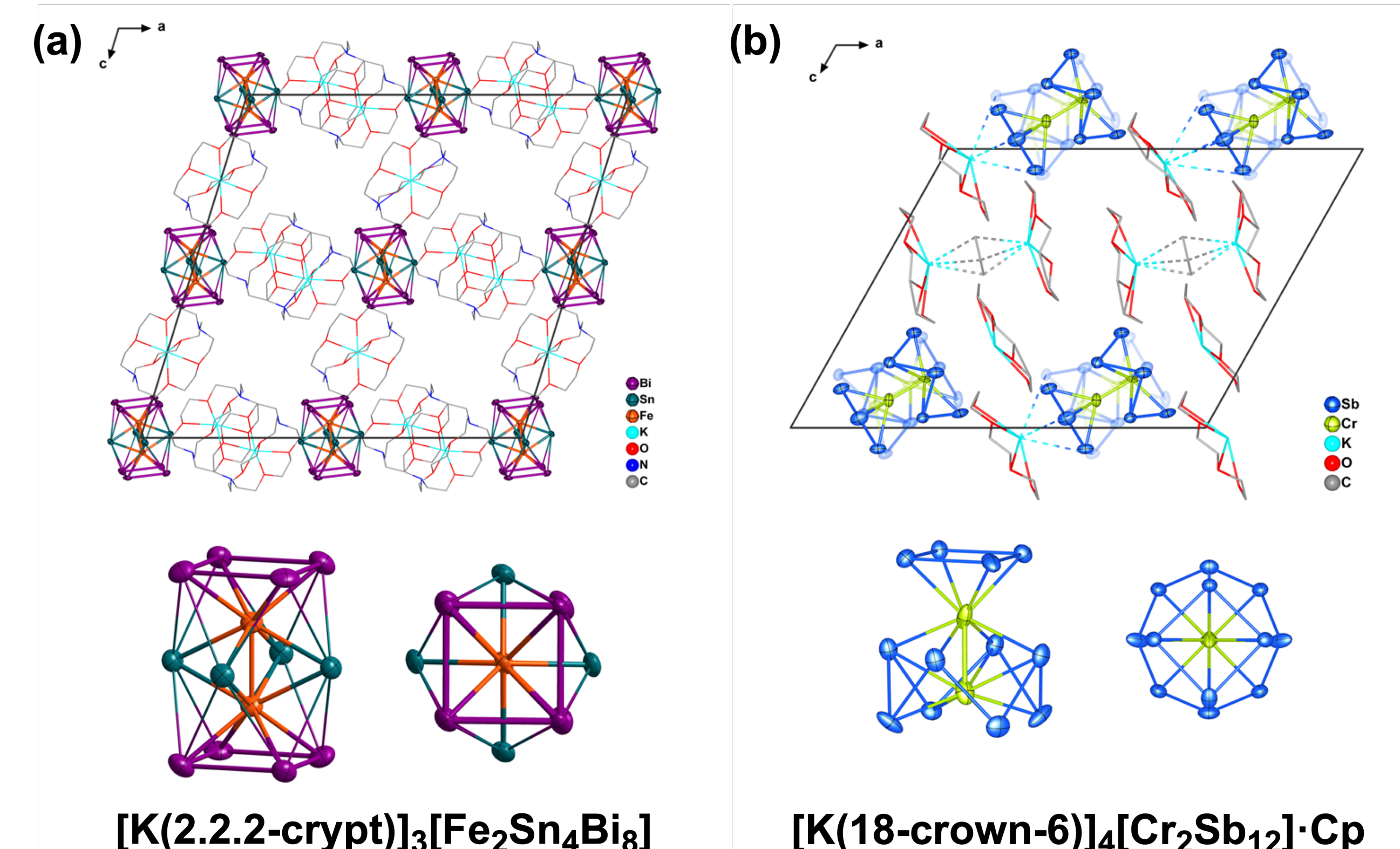
Introduction

- Endohedral Zintl clusters with 12 vertices adopt a range of architectures, including deltahedron,¹ triple-decker,² three-connected,³ and donut-like,⁴ depending on the identity of the encapsulated transition metal fragment.



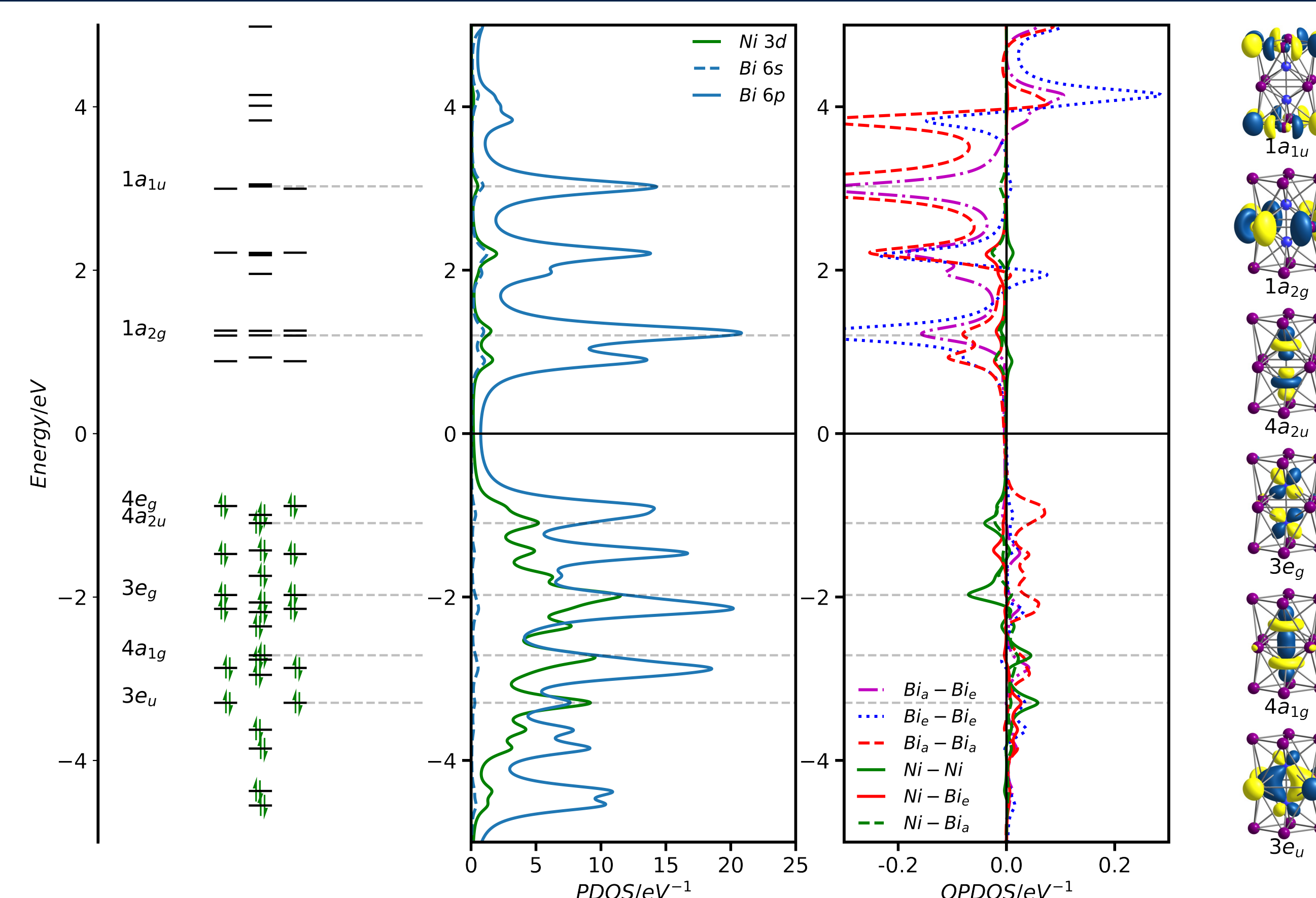
- We report two new members of the metal dimer encapsulated triple-decker family, D_{4h} - $[Fe_2Sn_4Bi_8]^{3-}$ and C_{4v} - $[Cr_2Sb_{12}]^{3-}$, both of which have 75 valence electrons and hence open shells.

Experimental and Computational Methods



- $[K(2.2.2\text{-crypt})]_2[Sn_2Bi_2] + DPPF \rightarrow [K(2.2.2\text{-crypt})]_3[Fe_2Sn_4Bi_8]$ (20% yield based on DPPF). Crystal structure is shown in (a).
- $K_3Sb_7 + 18\text{-crown-6} + CrCp_2 \rightarrow [K(18\text{-crown-6})]_4[Cr_2Sb_{12}] \cdot Cp$ (31% yield based on CrCp₂). Crystal structure is shown in (b).
- All calculations were performed with the Amsterdam Density Functional (ADF) package. PBE/TZ2P/ZORA level was used. The COSMO solvation model was applied to simulate the confined crystal environment.

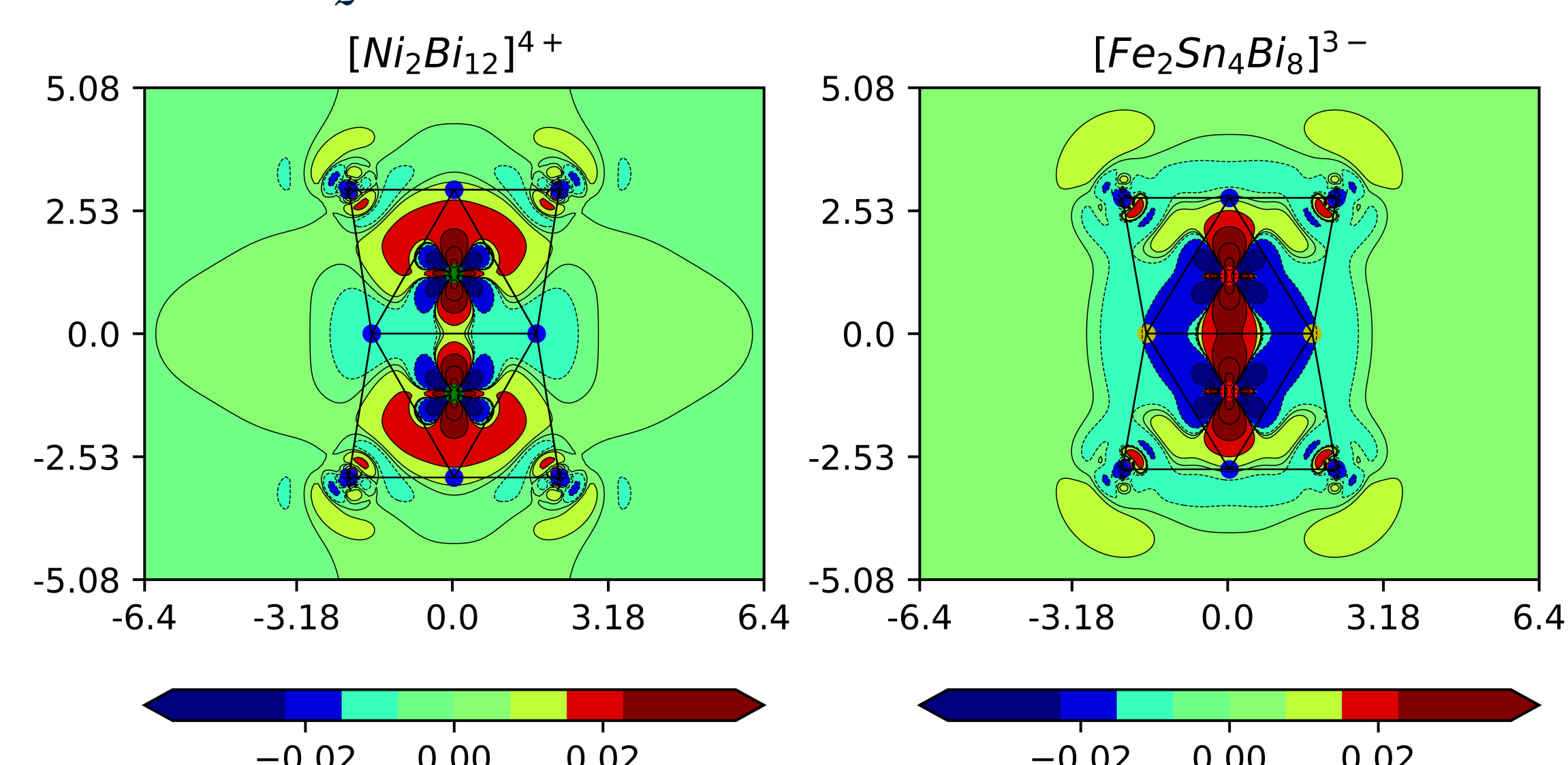
A Reference Point - 76-electron D_{4h} - $[Ni_2Bi_{12}]^{4+}$



- The Ni 3d band (green line) is underneath the Fermi level. The nickels are in core-like d^{10} configurations.
- The large HOMO-LUMO gap is indicative of its stability, suggesting 56 electrons are required to form the triple-decker cage (Bi_{12}^{4+}).

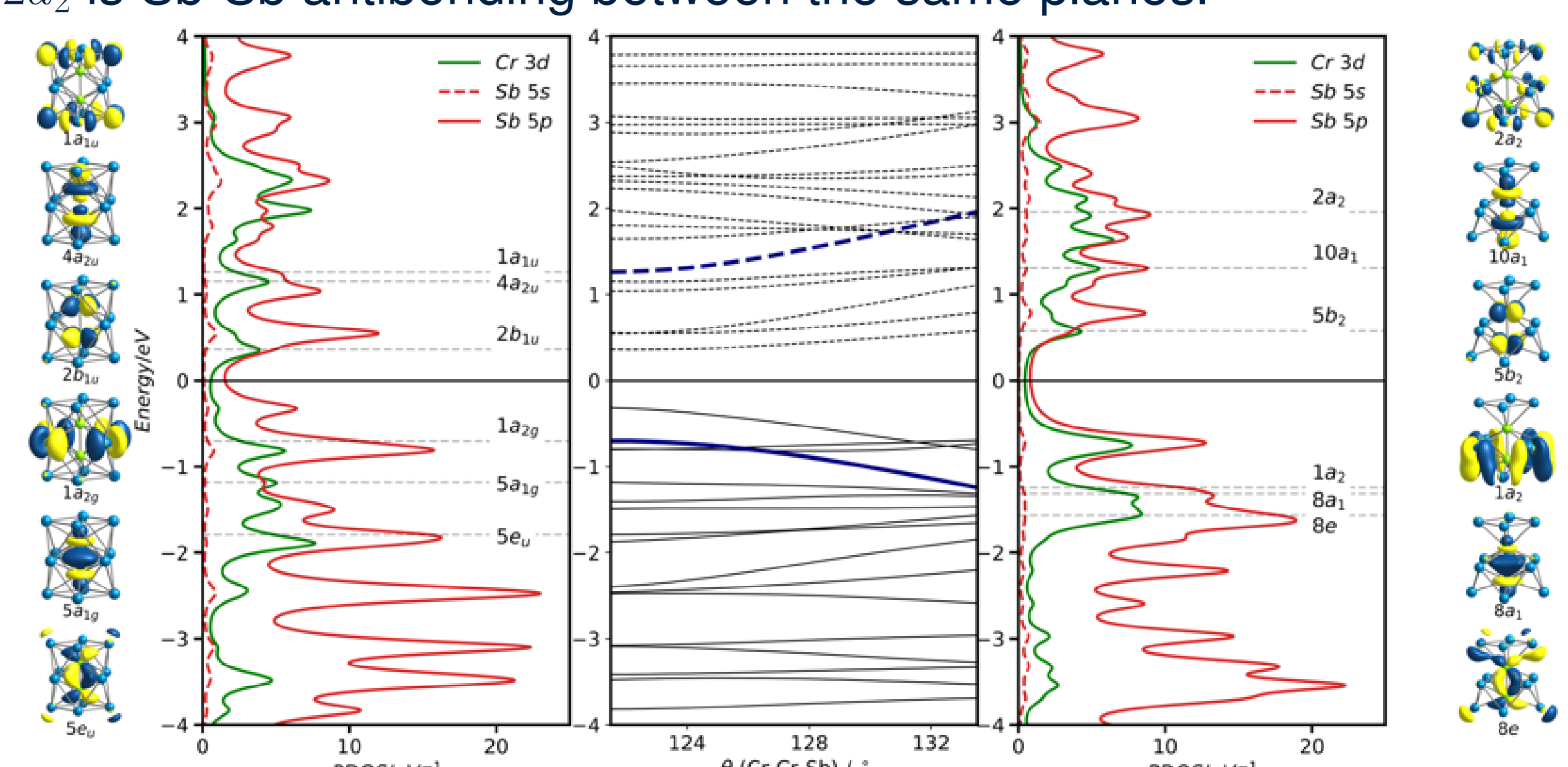
75-electron - D_{4h} - $[Fe_2Sn_4Bi_8]^{3-}$

- Compared to $[Ni_2Bi_{12}]^{4+}$, one electron is removed from Fe-Fe σ anti-bonding orbital. The electron count on the cage remains 56.
- In $[Fe_2Sn_4Bi_8]^{3-}$, the back-bonding from Fe-Fe π^* orbitals to Bi leading to charge accumulation at the pole and depletion around irons. In contrast, in $[Ni_2Bi_{12}]^{4+}$, reorganisation of electron density happens mainly between the $3d_{z^2}$ and $4s$ orbitals.



75-electron - C_{4v} - $[Cr_2Sb_{12}]^{3-}$

- From $[Fe_2Sn_4Bi_8]^{3-}$ to $[Cr_2Sb_{12}]^{3-}$, two electrons in the spin- α Cr-Cr σ antibonding orbital and the spin- β Cr-Cr δ antibonding orbital are transferred to the equatorial Sb-Sb antibonding orbital.
- A Walsh diagram for $[Cr_2Sb_{12}]^{3-}$ linking the D_{4h} and C_{4v} -symmetric forms shows a stabilization of $1a_2$ and concomitant destabilization of $2a_2$. The $1a_2$ orbital becomes bonding between the lower and middle Sb₄ planes, forming the eight Sb-Sb bonds of the crown-like Sb₈ unit while $2a_2$ is Sb-Sb antibonding between the same planes.



Conclusion

- The metal d orbitals are shifted upwards relative to those on the cage as we move from Ni to Fe and then to Cr.
- From $[Ni_2Bi_{12}]^{4+}$ to $[Fe_2Sn_4Bi_8]^{3-}$, the upward shift in the 3d orbitals leads to increased back-bonding from the metal to the cage, but the gross structure is otherwise unperturbed.
- For $[Cr_2Sb_{12}]^{3-}$, the occupied metal 3d orbitals move above the equatorial Sb-Sb antibonding $1a_{2g}$ orbital, leading to a two-electron reduction of the E_{12} cluster with concomitant oxidation of the Cr₂ unit. The occupation of the $1a_{2g}$ orbital triggers a second-order Jahn-Teller instability that drives the distortion from D_{4h} to C_{4v} .

References

- [1] Esenturk, E. N.; Fettinger, J.; Eichhorn, B. *J. Am. Chem. Soc.* **2006**, *128* (28), 9178–9186.
- [2] Groh, M. F.; Müller, U.; Isaeva, A.; Ruck, M. Z. *Anorg. Alig. Chem.* **2019**, *645*, 161–169.
- [3] Espinoza-Quintero, G.; Duckworth, J. C. A.; Myers, W. K.; McGrady, J. E.; Goicoechea, J. M. *J. Am. Chem. Soc.* **2014**, *136* (4), 1210–1213.
- [4] Min, X.; Popov, I. A.; Pan, F. X.; Li, L. J.; Matito, E.; Sun, Z. M.; Wang, L. S.; Boldyrev, A. I. *Angew. Chem., Int. Ed.* **2016**, *55* (18), 5531–5535.